Photon-electron polarization correlations in high-Z np_J-subshell photoionization

Young Soon Kim
Department of Physics, Myong-Ji University, Yong-In 449-728, Korea

I. B. Goldberg
Racah Institute of Physics, Hebrew University of Jerusalem, Jerusalem 91904, Israel

R. H. Pratt
Department of Physics and Astronomy, University of Pittsburgh, Pittsburgh, Pennsylvania 15260
(Received 12 July 1993)

A comprehensive survey is presented of the behavior of all correlations C_{ij} between the polarization of the incoming photon and the spin of the outgoing photoelectron, for ejection from all np_J subshells of uranium for photoelectron energies ranging from 1 eV to 100 keV. The numerical results for these polarization correlations are obtained within the independent-particle approximation in a relativistic self-consistent atomic field. At low photon energies the dipole predictions are generally valid, predicting large degrees of spin polarization of photoelectrons down to the threshold for all np_J subshells with a specific J, even for the outer shells where the spin-orbit coupling is weak. At some energies where the dipole correlations vanish, deviations from dipole predictions may be visible even at low photon energies. As the photon energy grows higher, multipoles eventually dominate and the dipole-type symmetry in the ejection angle is lost, while the curves of a given correlation for the initial states with the same total and orbital angular momenta and different n merge into a common curve. We also discuss the comparison with the usual nonrelativistic dipole limit, in which summing over the $J=\frac{1}{2}$ and $J=\frac{3}{2}$ substates results in np photoionization with no spin polarization. In the relativistic case the spin-orbit effects, magnified in the differences in the positions of Cooper minima for the outer shells at low energies, lead to finite spin polarization of photoelectrons even after summing over J.

PACS number(s): 32.80.Fb

I. INTRODUCTION

We wish to report here theoretical results for photon-photoelectron polarization correlations in $np_{\frac{1}{2}}$- and $np_{\frac{3}{2}}$-subshell photoionization of uranium, for photoelectron energies from 1 eV to 100 keV, obtained within an independent-particle approximation (IPA) in a relativistic self-consistent atomic field (Dirac-Slater type), including all significant multipole contributions. Experimental interest in the "complete" description of photoionization has been increasing in recent years with development of new synchotrons. Some references on other theoretical work in dipole approximation as well as on actual measurements of photoelectron spin polarization are given in our previous paper [1]. This paper continues the program of work begun in our recent report on polarization correlations in ns-subshell photoionization of uranium [1], based on the characterization of Refs. [2,3]. Previously we investigated total cross sections and angular distributions in the same IPA scheme [4,5]. Our numerical results here are obtained with the procedures described in these papers. For inner shells and high electron energies where IPA is known to work well, this numerical procedure may give quantitatively reliable results within a few percent, while it is only qualitative for outer shells and low energies. These results are expected to be generic for all the high-Z elements (uranium is a good representative of a high-Z element within IPA).

We observe many novel features here in the np correlations which were not seen in ns cases, mainly reflecting the fact that there is only one J ($=\frac{1}{2}$) subshell for $L=0$. These novel features (though not their quantitative details at low energies) may be expected to persist beyond IPA, since they result from the existence of more channels and the existence of Cooper minima, both very general properties of the matrix elements.

The correlations between the specified polarization of the incoming photon (described with Stokes parameters ξ_i) and a specified spin measurement direction for the ejected electron in its rest frame (specified by the unit vector $\zeta=\langle\chi|\sigma|\chi\rangle$ where $|\chi\rangle=\zeta\cdot\sigma|\chi\rangle$) are again characterized by the coefficients C_{ij}, as in Refs. [1–3], as functions of angle and energy. These correlations specify the cross section for emission of the photoelectron with the specified direction of the spin measurement, in absorption of the photon of the specified polarization state,

$$\frac{d\sigma(\xi,\zeta)}{d\Omega}=\left[\frac{d\sigma}{d\Omega}\right]_{\text{unpol}}\left[\frac{1}{2}\sum_{i,j=0}^{3}\xi_i\zeta_j C_{ij}\right]. \tag{1}$$

Here $\xi_0=\zeta_0=C_{00}\equiv 1$; $(d\sigma/d\Omega)_{\text{unpol}}$ is the photoelectron angular distribution from unpolarized photons and no spin measurement. As in the ns studies, it is assumed that the initial bound state of the target atom is unpolar-

ized and that the polarization of the residual ion is not observed.

We note similarities and differences between the correlations C_{ij} of *ns*- and np_J-subshell photoionization. For the low-energy outer-shell (LEOS) cases, i.e., for photoionization of outer subshells with low photon energies, the dipole formalism gives the general features of the C_{ij} for np_J cases, with radial matrix elements and phase-shift differences of dipole channels, as it had for *ns* cases of uranium. For other elements, especially for intermediate Z such as tin, correction terms beyond dipole approximation may be visible even for LEOS cases near Cooper minima [6]. For inner *ns* shells, nondipolar effects may persist down to threshold even for low and intermediate Z elements, as shown in our K- and L-shell studies [7,8]. But unlike the *ns* cases, where significant low-energy correlations varying in energy are only found near dipole Cooper minima separated due to the spin-orbit coupling, large degrees of spin polarization are predicted down to the threshold for the photoelectrons from np_J with a specific J, varying with energy. For *ns* correlations the amplification of the correction terms beyond the dipole approximation tends to occur near dipole Cooper minima in those cases for which the separation of matrix element zeros due to the spin-orbit coupling is not large, as for intermediate Z [6]. On the other hand, low-energy deviations from the dipole predictions for np_J subshells may rather be seen away from Cooper minima, as we shall discuss later. At low energies, full multipole results, as well as relativistic dipole results after summed over J, resemble the usual J-summed nonrelativistic dipole expectations of vanishing photoelectron spin polarization. Deviations occur at high photon energies or near dipole Cooper minima.

As photon energy becomes higher the C_{ij} deviate from dipole predictions due to the growing higher multipole contributions. For given energy the curves of a given C_{ij} with different n for a given $K \equiv (-1)^{J+L+1/2}(J+\frac{1}{2})$ have practically merged into a common curve by the time the photoelectron kinetic energy ε becomes as high as 100 keV, while the shape of the common curves as functions of the ejection angle θ continues to change with ε.

In Sec. II we give the basic equations relating the polarization correlation coefficients C_{ij} to the more obvious quantity P_α, the degree of spin polarization, measured along the direction α, of the beam of photoelectrons emitted into a specified solid angle in absorption of a beam of photons of specified polarization properties. In Sec. III we give the five dipole parameters of the so-called "complete" description of photoionization in the long-wavelength limit, as in Ref. [1], and present the correlation coefficients C_{ij} for np_J photoionization in terms of these dipole parameters in the same limit. The full numerical results as well as their deviations from dipole predictions are given and discussed in Sec. IV.

II. BASIC EQUATIONS

Equations (1), (2), and (5)–(10) are generally valid for any type of the photon polarization, and before we introduce our choice of the coordinate axes the equations are independent of the coordinate system [through Eq. (5)]. As in our *ns* studies, it is assumed that the initial bound state of the target atom is unpolarized and that the polarization of the residual ion is not observed. Note that the usual photoelectron angular distribution resulting from absorption of a photon of a definite polarization ξ and no spin measurement is

$$\frac{d\sigma(\xi)}{d\Omega} = \frac{d\sigma(\xi,\zeta)}{d\Omega} + \frac{d\sigma(\xi,-\zeta)}{d\Omega} , \tag{2}$$

where the result is independent of the choices of ζ and $-\zeta$ for the photoelectron spin measurement direction. The differential cross section with the spin of the photoelectrons measured along ζ, resulting from an unpolarized beam of photons is

$$\frac{d\sigma(\zeta)}{d\Omega} = \frac{1}{2}\left[\frac{d\sigma(\xi,\zeta)}{d\Omega} + \frac{d\sigma(-\xi,\zeta)}{d\Omega}\right] , \tag{3}$$

independent of the choice of ξ. Finally

$$\left[\frac{d\sigma}{d\Omega}\right]_{\text{unpol}} = \frac{d\sigma(\zeta)}{d\Omega} + \frac{d\sigma(-\zeta)}{d\Omega} = \frac{1}{2}\left[\frac{d\sigma(\xi)}{d\Omega} + \frac{d\sigma(-\xi)}{d\Omega}\right] \tag{4}$$

is the differential cross section for emission of photoelectrons into solid angle $d\Omega$, not determining their spin direction, on absorption of an unpolarized beam of photons. Equation (4) does not depend on the directions ζ and ξ. The degree of spin polarization measured along a certain direction ζ at a particular ejection angle θ from an incident photon beam characterized by ξ becomes

$$P_\zeta(\theta) = \frac{N_\uparrow - N_\downarrow}{N_\uparrow + N_\downarrow} = \frac{\dfrac{d\sigma(\xi,\zeta)}{d\Omega} - \dfrac{d\sigma(\xi,-\zeta)}{d\Omega}}{\dfrac{d\sigma(\xi,\zeta)}{d\Omega} + \dfrac{d\sigma(\xi,-\zeta)}{d\Omega}} , \tag{5}$$

where $N_\uparrow$ ($N_\downarrow$) is the number of electrons ejected into the solid angle $d\Omega$ detected with spin up (down) along the direction ζ.

The coordinate system employed here, as well as in our earlier work for *ns* cases, is shown in Fig. 1, which is the same as Fig. 1 of Ref. [1]. Here $\mathbf{k}$ defines the $\hat{\mathbf{z}}$ axis and the production plane is the $\hat{\mathbf{x}}$-$\hat{\mathbf{z}}$ plane. Note that the $\hat{\mathbf{x}}$ axis is chosen to lie in the production plane so that the azimuthal angle ϕ dependence of the process with linearly polarized photons is carried by the Stokes parameters. In this characterization we need to deal with a smaller number of angular parameters, without any loss of generality, than for example in Ref. [9] or [10]. The only inconvenience, if any, is that the Stokes parameters are defined after the choice of direction of observation of $\mathbf{p}$ of the ejected photoelectron, due to our choice of the $\hat{\mathbf{x}}$ axis as in the production plane. The definitions of the Stokes parameters ξ_i for a given photon in terms of the photon polarization vector $\boldsymbol{\epsilon} = \epsilon_1\hat{\mathbf{x}} + \epsilon_2\hat{\mathbf{y}}$ are given below, as well as the components of ζ along the axes $(\hat{\mathbf{1}},\hat{\mathbf{2}},\hat{\mathbf{3}})$ obtained by rotating $(\hat{\mathbf{x}},\hat{\mathbf{y}},\hat{\mathbf{z}})$ through the ejection angle θ between the two momenta $\mathbf{p}$ and $\mathbf{k}$ of the electron and photon,

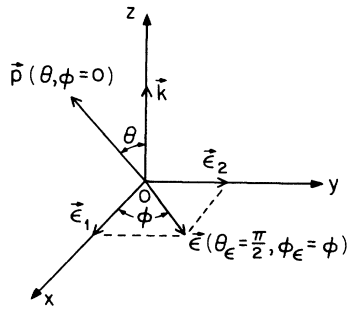

FIG. 1. Coordinate system employed in this work.

around the $\hat{\mathbf{y}}$ axis. $\hat{\mathbf{y}}=\hat{\mathbf{2}}$ is along the direction of $\mathbf{k}\times\mathbf{p}$; $\hat{\mathbf{3}}$ is along $\mathbf{p}$ and $\hat{\mathbf{1}}$ is also in the production plane. The photoelectron spin is characterized either as longitudinal or as transverse in or out of the production plane. Another useful choice of the z axis when the incoming photons are linearly polarized is along the photon polarization vector ϵ. The relation between these two choices is discussed in detail in Ref. [7]. Here we have

$$\begin{aligned}\xi_1&=\epsilon_1^*\epsilon_1-\epsilon_2^*\epsilon_2\ ,\\ \xi_2&=\epsilon_1^*\epsilon_2+\epsilon_2^*\epsilon_1\ ,\\ \xi_3&=i(\epsilon_2^*\epsilon_1-\epsilon_1^*\epsilon_2)\ ,\end{aligned}\tag{6}$$

where for a single photon $\sum_{i=1}^3\xi_i^2=1$. The ξ corresponding to a partially polarized beam of photons are the average $\bar{\xi}$ over the ξ for individual photons and $\sum\bar{\xi}_i^2=P_{ph}\le 1$, where P_{ph} is the degree of partial polarization of the beam of photons. For the direction ζ of electron spin measurement,

$$\zeta_1=\boldsymbol{\zeta}\cdot(\hat{\mathbf{y}}\times\hat{\mathbf{p}}),\quad \zeta_2=\boldsymbol{\zeta}\cdot\hat{\mathbf{y}},\quad \zeta_3=\boldsymbol{\zeta}\cdot\hat{\mathbf{p}}\ .$$

Details of the coordinate system as well as the general physical meanings of the C_{ij} are also found in Ref. [1], but some simple examples may illuminate the basic structure of this description.

Most generally with our choice of the coordinate system, we have

$$\begin{aligned}\frac{d\sigma(\boldsymbol{\xi},\boldsymbol{\zeta})}{d\Omega}=\left[\frac{d\sigma}{d\Omega}\right]_{\text{unpol}}&\tfrac{1}{2}[1+\zeta_2C_{02}(\theta)+\xi_1C_{10}(\theta)\\ &+\xi_1\zeta_2C_{12}(\theta)+\xi_2\zeta_1C_{21}(\theta)\\ &+\xi_2\zeta_3C_{23}(\theta)+\xi_3\zeta_1C_{31}(\theta)\\ &+\xi_3\zeta_3C_{33}(\theta)]\ ,\end{aligned}\tag{7}$$

(see Refs. [2,3] for the symmetry argument for the seven possible nontrivial nonzero C_{ij}) and

$$\begin{aligned}P_l(\theta)\equiv P_3(\theta)&=\frac{\xi_2C_{23}(\theta)+\xi_3C_{33}(\theta)}{1+\xi_1C_{10}(\theta)}\ ,\\ P_{t1}(\theta)\equiv P_1(\theta)&=\frac{\xi_2C_{21}(\theta)+\xi_3C_{31}(\theta)}{1+\xi_1C_{10}(\theta)}\ ,\\ P_t(\theta)\equiv P_2(\theta)\equiv P_y(\theta)&=\frac{C_{02}(\theta)+\xi_1C_{12}(\theta)}{1+\xi_1C_{10}(\theta)}\ ,\end{aligned}\tag{8}$$

where

$$|\mathbf{P}(\theta)|=\left[\sum_{i=1}^3|P_i(\theta)|^2\right]^{\frac{1}{2}}\tag{9}$$

is the magnitude of the spin-polarization vector. Here the subscripts l, $t1$, and t stand for longitudinal, transverse in, and perpendicular to the production plane, respectively. Note that the denominator of Eq. (8) corresponds to the usual angular distribution of the photoelectrons in this coordinate system with a particular photon polarization, given by

$$\frac{d\sigma(\boldsymbol{\xi})}{d\Omega}=\left[\frac{d\sigma}{d\Omega}\right]_{\text{unpol}}[1+\xi_1C_{10}(\theta)]\ .\tag{10}$$

If the incoming photon beam is unpolarized, $\xi_1=\xi_2=\xi_3=0$ and the system has no intrinsic azimuthal-angle dependence. Since C_{02} is the only nonvanishing C_{0j} except for $C_{00}=1$, Eq. (1) together with Eq. (3) in this case gives

$$\frac{d\sigma(\boldsymbol{\zeta})}{d\Omega}=\left[\frac{d\sigma}{d\Omega}\right]_{\text{unpol}}\tfrac{1}{2}[1+\zeta_2C_{02}(\theta)]\ .\tag{11}$$

This indicates that partial transverse spin polarization perpendicular to the production plane will be the largest possible spin polarization that can be measured with unpolarized photons, since the difference between $d\sigma(\boldsymbol{\zeta})/d\Omega$ and $d\sigma(-\boldsymbol{\zeta})/d\Omega$ is maximized when the photoelectron spin is measured along the $\hat{\mathbf{y}}$ direction ($\zeta_2=+1$ or -1). The degree of transverse spin polarization perpendicular to the production plane $P_t(\theta)\equiv P_y(\theta)\equiv P_2(\theta)$ is equal to $C_{02}(\theta)$ in this case, from Eqs. (5) and (11) or directly from Eq. (8). If $C_{02}(\theta)$ at some particular ejection angle θ vanishes, the cross section is independent of spin direction and as many photoelectrons come out at this angle with spin "up" as with spin "down" along any direction, resulting in an unpolarized flux of photoelectrons.

For linear photon polarization, with ϵ making an angle ϕ from the $\hat{\mathbf{x}}$ axis, i.e., from the production plane, all the ϕ dependence is contained in the Stokes parameters

$$\begin{aligned}\xi_1&=\cos2\phi\ ,\\ \xi_2&=\sin2\phi\ ,\\ \xi_3&=0\ ,\end{aligned}\tag{12}$$

and no explicit azimuthal-angle dependence appears in our formulas, due to our choice of the $\hat{\mathbf{x}}$ axis. From Eq. (7) with Eq. (12), we have

$$\begin{aligned}\frac{d\sigma(\boldsymbol{\xi},\boldsymbol{\zeta})}{d\Omega}=\left[\frac{d\sigma}{d\Omega}\right]_{\text{unpol}}&\tfrac{1}{2}[1+\zeta_2C_{02}(\theta)+\xi_1C_{10}(\theta)\\ &+\xi_1\zeta_2C_{12}(\theta)+\xi_2\zeta_1C_{21}(\theta)\\ &+\xi_2\zeta_3C_{23}(\theta)]\ ,\end{aligned}\tag{13}$$

and from Eq. (8) with Eq. (12)

$$P_l(\theta)=\frac{\xi_2 C_{23}(\theta)}{1+\xi_1 C_{10}(\theta)} ,$$
$$P_{t1}(\theta)=\frac{\xi_2 C_{21}(\theta)}{1+\xi_1 C_{10}(\theta)} , \quad (14)$$
$$P_t(\theta)=\frac{C_{02}(\theta)+\xi_1 C_{12}(\theta)}{1+\xi_1 C_{10}(\theta)} ,$$

where the same denominator as before properly takes care of the total flux of photoelectrons coming out in a particular direction. In particular, when the photon polarization vector ϵ is along the $\hat{\mathbf{x}}$ or $\hat{\mathbf{y}}$ axis ($\epsilon_2=0$ or $\epsilon_1=0$, and $\phi=0$ or $\pi/2$, i.e., in or perpendicular to the production plane, respectively), which corresponds to observing the photoelectrons coming out in or making an angle θ with the plane made by ϵ and $\mathbf{k}$, we have $\xi_1=\pm 1$, respectively, and $\xi_2=0$. Again, the largest spin polarization will be observed when measured along $\hat{\mathbf{y}}$, and

$$P_t(\theta)=\frac{C_{02}\pm C_{12}(\theta)}{1\pm C_{10}(\theta)} .$$

In the relativistic dipole approximation, as we will see below, $C_{02}(\theta)=C_{12}(\theta)$ and an unpolarized photoelectron flux is expected to be observed at all angles θ when the production plane is perpendicular to ϵ.

When the linear polarization vector ϵ of photons makes an angle $\pm\pi/4$ with the $\hat{\mathbf{x}}$ axis ($\epsilon_1=\pm\epsilon_2$), we have $\xi_2=\pm 1$, respectively, and $\xi_1=0$ in Eq. (13). This results in the degree of longitudinal spin polarization $P_l(\theta)\equiv P_3(\theta)=\pm C_{23}(\theta)$ from Eq. (14), which (as we will see below) is zero in the dipole case. This gives the degrees of transverse spin polarization in and perpendicular to the production plane $P_{t1}(\theta)\equiv P_1(\theta)=\pm C_{21}(\theta)$ and $P_t(\theta)=C_{02}(\theta)$, respectively.

For elliptically polarized photons, ϵ is complex and we have ξ_3 and at least one of ξ_1 and ξ_2 nonzero from Eq. (6). With circularly polarized photons, $\xi_3=\pm 1$ and $\xi_1=\xi_2=0$, and again we have no intrinsic dependence on the azimuthal angle:

$$\frac{d\sigma(\xi,\zeta)}{d\Omega}=\left[\frac{d\sigma}{d\Omega}\right]_{\text{unpol}}\tfrac{1}{2}[1+\zeta_2 C_{02}(\theta)\pm\zeta_1 C_{31}(\theta) \pm\zeta_3 C_{33}(\theta)] , \quad (15)$$

and from Eq. (8)

$$P_l(\theta)=\pm C_{33}(\theta) ,$$
$$P_{t1}(\theta)=\pm C_{31}(\theta) , \quad (16)$$
$$P_t(\theta)=C_{02}(\theta) .$$

We have introduced all seven nontrivial C_{ij} in the above examples. ($C_{00}\equiv 1$ and the other $C_{ij}=0$.) For a partially polarized flux of photons Eqs. (7) and (8) are valid with $\bar{\xi}_i$ in places of ξ_i. (Actually, partially polarized beams of photons may be written as a sum of unpolarized and polarized photon beams with appropriate weight, or equivalently, the size of the Stokes parameters defined for the polarized part of the beam may simply be reduced by a factor of the partial photon polarization P_{ph}.) Note that Eqs. (13) and (15) reduce to Eq. (11) via Eq. (4), for the unpolarized photon flux is indeed an uncorrelated sum of the two orthogonal photon polarizations with equal weight.

III. DIPOLE FORMS OF POLARIZATION CORRELATIONS

The procedure to reduce the full multipole formalism to their dipole forms for the C_{ij} for ns-subshell photoionization was given in Ref. [1] in some detail. Here for np_J-subshells we will give only the resulting reduced dipole forms for C_{ij} in terms of the five dipole parameters. For brevity, we write the radial dipole matrix elements and continuum phase shifts as follows:

$$R_1^{2J}\equiv R(np_J\rightarrow\varepsilon s_{1/2}) ,$$
$$R_3^{2J}\equiv R(np_J\rightarrow\varepsilon d_{3/2}) , \quad (17)$$
$$R_5^{3}\equiv R(np_{3/2}\rightarrow\varepsilon d_{5/2}) ,$$

where $J=\frac{1}{2}$ or $\frac{3}{2}$ and

$$\delta_1\equiv(\text{phase shift of } \varepsilon s_{1/2}) ,$$
$$\delta_3\equiv(\text{phase shift of } \varepsilon d_{3/2}) , \quad (18)$$
$$\delta_5\equiv(\text{phase shift of } \varepsilon d_{5/2}) ,$$
$$\delta_{ij}\equiv\delta_i-\delta_j . \quad (19)$$

As in Ref. [1], in dipole approximation the physical content of the photoeffect matrix element is expressed in terms of five physically measurable dipole parameters: the reduced cross section $\bar{\sigma}$, the asymmetry parameter β for the photoelectron angular distribution, the transverse spin-polarization parameter η for the photoelectrons (resulting from unpolarized or linearly polarized photons), and the transverse and longitudinal spin-polarization parameters ξ and ζ, respectively (resulting from circularly polarized photons).

(a) For $np_{1/2}$ cases,

$$\bar{\sigma}=(R_1^{\frac{1}{2}})^2+2(R_3^{\frac{1}{2}})^2 ,$$
$$\beta=2[(R_3^{\frac{1}{2}})^2+2R_1^{\frac{1}{2}}R_3^{\frac{1}{2}}\cos\delta_{13}]/\bar{\sigma} ,$$
$$\eta=-3R_1^{\frac{1}{2}}R_3^{\frac{1}{2}}\sin\delta_{13}/\bar{\sigma} , \quad (20)$$
$$\zeta=[(R_1^{\frac{1}{2}})^2+(R_3^{\frac{1}{2}})^2-2R_1^{\frac{1}{2}}R_3^{\frac{1}{2}}\cos\delta_{13}]/\bar{\sigma}=1-\frac{\beta}{2} ,$$
$$\xi=[-(R_1^{\frac{1}{2}})^2+2(R_3^{\frac{1}{2}})^2-R_1^{\frac{1}{2}}R_3^{\frac{1}{2}}\cos\delta_{13}]/\bar{\sigma} ,$$

where only three parameters are independent (as in the ns cases) since only two different continuum states $\varepsilon s_{1/2}$ and $\varepsilon d_{3/2}$ can be reached via an $E1$ transition, and therefore only one phase-shift difference and two radial matrix elements occur. We use the same nomenclature as in Ref. [9] for the dipole parameters; it should be clear enough from context not to confuse ξ and ζ with ξ_i or ζ_j. Note that the expressions are almost identical to those of the ns cases, except for an overall minus sign for η and ξ. However, there R_1 and R_3 are the transitions from ns to $\varepsilon p_{1/2}$

and to $\varepsilon p_{3/2}$, respectively; without spin-orbit interaction in the continuum, $R_1=R_3$ and $\delta_{13}=0$ resulting in $\eta=\zeta=\xi=0$ (no spin polarization of photoelectrons) and $\beta=2$. On the other hand, R_1^1 and R_3^1 here are the transitions from $np_{1/2}$ to the $\varepsilon s_{1/2}$ and $\varepsilon d_{3/2}$ continuum states, respectively, and δ_{13} is the corresponding difference, resulting in significant spin polarizations varying with energy. This is due to the different energy dependences of the wave functions and phase shifts of the two different partial waves εs and εd.

(b) For $np_{3/2}$ cases, all five dipole parameters are independent, since there are three different continuum states $\varepsilon s_{1/2}$, $\varepsilon d_{3/2}$, and $\varepsilon d_{5/2}$, and hence two phase-shift differences and three radial matrix elements occur in the dipole approximation:

$$
\begin{aligned}
\bar{\sigma}&=2((R_1^3)^2+\tfrac{1}{5}(R_3^3)^2+\tfrac{9}{5}(R_5^3)^2)\ ,\\
\beta&=(-\tfrac{8}{25}(R_3^3)^2+\tfrac{72}{25}(R_5^3)^2+\tfrac{4}{5}R_1^3R_3^3\cos\delta_{13}+\tfrac{36}{5}R_1^3R_5^3\cos\delta_{15}+\tfrac{36}{25}R_3^3R_5^3\cos\delta_{35})/\bar{\sigma}\ ,\\
\eta&=(-\tfrac{3}{5}R_1^3R_3^3\sin\delta_{13}+\tfrac{18}{5}R_1^3R_5^3\sin\delta_{15}+\tfrac{9}{5}R_3^3R_5^3\sin\delta_{35})/\bar{\sigma}\ ,\\
\zeta&=(-(R_1^3)^2+\tfrac{2}{25}(R_3^3)^2+\tfrac{27}{25}(R_5^3)^2+2R_1^3R_3^3\cos\delta_{13}-\tfrac{54}{25}R_3^3R_5^3\cos\delta_{35})/\bar{\sigma}\ ,\\
\xi&=((R_1^3)^2+\tfrac{4}{25}(R_3^3)^2-\tfrac{81}{25}(R_5^3)^2+R_1^3R_3^3\cos\delta_{13}+\tfrac{27}{25}R_3^3R_5^3\cos\delta_{35})/\bar{\sigma}\ .
\end{aligned}
\tag{21}
$$

In terms of these parameters we have in the dipole case

$$C_{02}=-\eta\sin\theta\cos\theta/D_{00}\ , \tag{22}$$

$$C_{10}=\tfrac{3}{4}\beta\sin^2\theta/D_{00}\ , \tag{23}$$

$$C_{12}=C_{02}\ , \tag{24}$$

$$C_{21}=\eta\sin\theta/D_{00}\ , \tag{25}$$

$$C_{23}=0\ , \tag{26}$$

$$C_{31}=\xi\sin\theta/D_{00}\ , \tag{27}$$

$$C_{33}=\zeta\cos\theta/D_{00}\ , \tag{28}$$

where

$$D_{00}\equiv 1-\tfrac{1}{2}\beta P_2(\cos\theta)\ . \tag{29}$$

Note that $\bar{\sigma}D_{00}$ is essentially $(d\sigma/d\Omega)_{\text{unpol}}$ apart from an overall energy-dependent factor depending on the normalization of the continuum wave functions ($k/16\pi pE\alpha$ in our case), which is irrelevant to evaluation of C_{ij}. It is easy to see that with the spin-orbit interaction neglected, $R_3^1=R_3^3=R_5^3$ becomes $R(np\rightarrow\varepsilon d)$ and $\delta_3=\delta_5$ becomes δ_d since the wave functions of the $np_{1/2}$ and $np_{3/2}$ states are the same, and those of the $\varepsilon d_{3/2}$ and $\varepsilon d_{5/2}$ are same. Hence the reduced subshell cross section $\bar{\sigma}$ for $np_{3/2}$ becomes twice that for $np_{1/2}$ (the statistical branching ratio), the asymmetry parameter β for the angular distribution becomes identical in the two cases, and the polarization parameters η, ζ, and ξ for $np_{3/2}$ becomes $(-\frac{1}{2})$ times those of $np_{1/2}$, respectively. Hence C_{ij} for $np_{3/2}$ become $(-\frac{1}{2})$ times C_{ij} for $np_{1/2}$ except for $C_{00}=1$ and C_{10} which is independent of the spin polarization of the photoelectrons. In this limit of vanishing spin-orbit coupling, therefore, one expect a complete cancellation of the spin polarization when summed over J, since the weighting factors are 2:1 and the polarizations are -1:2. We discuss the deviations from this nonrelativistic limit in Sec. IV in more detail.

IV. RESULTS AND DISCUSSIONS

Figures 2–8 show the calculated results for the seven nontrivial C_{ij} as functions of θ, for all np_J subshells of uranium with photoelectron energies from 1 eV to 100 keV. Lower panels are for $np_{1/2}$ and the upper panels for $np_{3/2}$. In Figs. 9 and 10 we show the radial dipole matrix elements R_{2j}^{2J} and the phase-shift differences δ_{1j} as defined in Eqs. (17)–(19), as functions of photoelectron kinetic energy ε, and in Fig. 11 we show the resulting dipole parameters. We will see that the features in the dipole radial matrix elements (such as dipole Cooper minima) and in the phase-shift differences (as, for example, going through zero or π) are clearly reflected in the dipole parameters, which in turn mainly determine the behavior of C_{ij} in LEOS.

Dipole Cooper minima play an important role here, as in the photoelectron angular distributions or in the polarization correlations of ns cases. From Eq. (20) we see that when $R_3^1=0$ (a dipole Cooper minimum of the $np_{1/2}\rightarrow\varepsilon d_{3/2}$ channel), $\beta=\eta=0$ and $\zeta=-\xi=1$, as we observe for $5p_{1/2}$ and $6p_{1/2}$ at about 160 eV and 270 eV, respectively, from Figs. 9 and 11. This results in $C_{31}=-\sin\theta$ and $C_{33}=\cos\theta$ with all the other $C_{ij}=0$ except C_{00}. From Eqs. (9) and (16) we expect at these energies that photoelectrons are completely polarized along the direction making an angle θ with the $\hat{3}$-axis in the production plane. (Similar situations can occur with autoionizing resonances, as was measured and discussed by Böwering *et al.* for a $^1S_0$ autoionizing resonance of Tl^+ [11].)

For $np_{3/2}$ cases, the largest possible magnitude of the spin-polarization vector is $\frac{1}{2}$ as the ratio of the dipole parameters of $np_{1/2}$ and $np_{3/2}$ cases is -2. Also, there are two $np_{3/2}\rightarrow\varepsilon d$ channels and the corresponding Cooper minima are separated in energy [12], making the feature of maximum spin polarization near dipole Cooper minima less clear.

Note that C_{ij} for $J=\frac{1}{2}$ are not exactly -2 times that

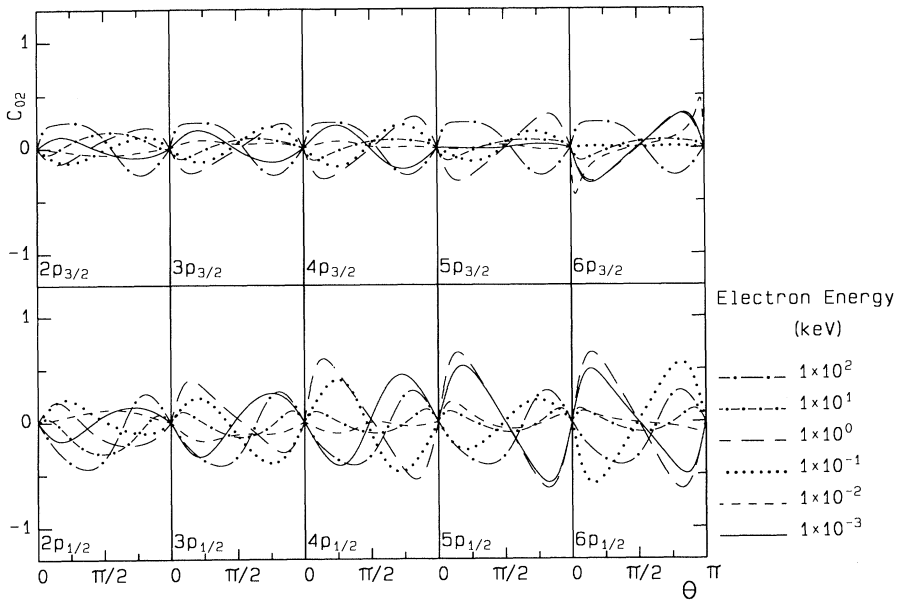

FIG. 2. Full multipole results for C_{02}.

for $J=\frac{3}{2}$ especially at high energies, for inner shells, or when Cooper minima are present.

Figures 12–18 show the differences between the full multipole results and the dipole ones. The arrangement of these figures are such that the n dependence at a given photoelectron energy may be examined easily so that we can again emphasize the merging of the curves at high photoelectron energies for each C_{ij} for the initial states with a given K, i.e., with a given (L,J), and different n. As we pointed out in our previous papers [1,5], this feature of common curves is due to the fact that at high energies the transition matrix elements are determined at short distances where all the bound wave functions of the same K and different n tend to have the same radial wave-function shape. The radial wave function for the lowest n state starts to deviate first from the common shape, hence the correlation coefficients (or the angular distribution parameters) from the common curve.

Note that the asymmetries of the correlation curves in Figs. 2–8 about $\theta=\pi/2$ are entirely due to these differences coming from the higher multipole contributions. These deviations from the dipole predictions are larger for C_{ij} of $np_{1/2}$ than $np_{3/2}$ at the same photoelectron energy, partly because the photon energy is higher due to the larger binding energy, but mainly because the full multipole results also maintains the (-2):1 feature; if the fractional deviation is similar the absolute difference for $np_{1/2}$ itself is about (-2) times that for $np_{3/2}$.

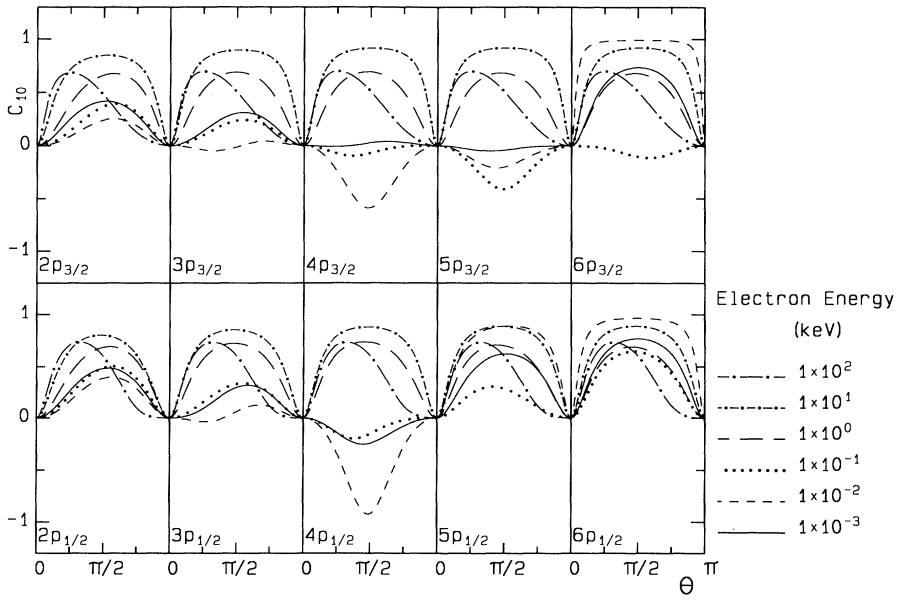

FIG. 3. Full multipole results for C_{10}.

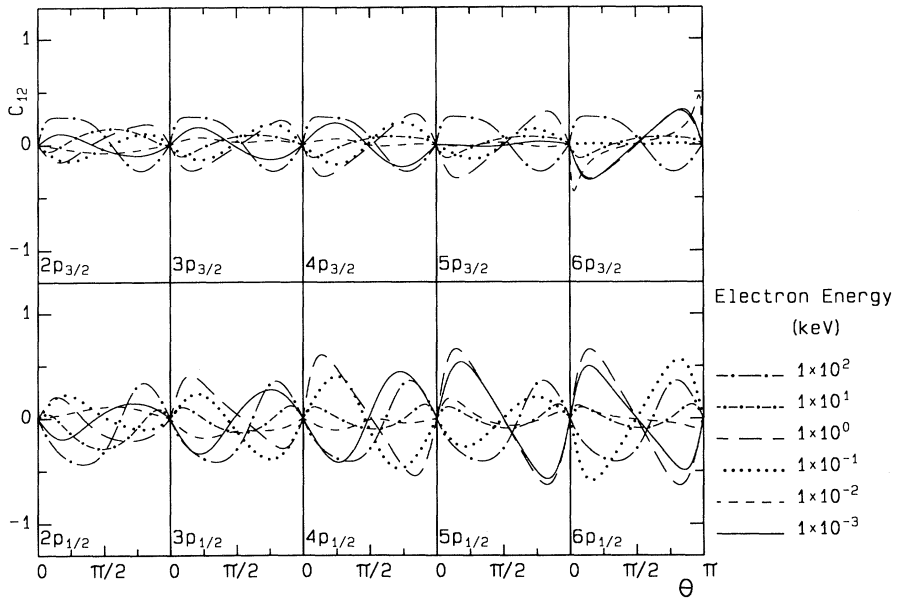

FIG. 4. Full multipole results for C_{12}.

Since the absolute values of the differences are less than 0.1 in most of the LEOS cases, close examination of Eqs. (20)–(28) together with Figs. 2–11 gives us a general understanding of the behavior of C_{ij} in LEOS in terms of the dipole parameters, or in terms of the dipole matrix elements and phase shifts. For LEOS cases we note from Figs. 12–18 that the deviations are relatively small except at $\varepsilon=10$ eV. At this energy we note that the multipole results for C_{02}, C_{12}, and C_{21} (which are proportional to η in their dipole forms) and C_{23} (which is zero in the dipole form) deviate more from their dipole expectations (zero) than at other energies, and than C_{31} and C_{33} which do not involve η. A similar situation again occurs at 10 keV. Note from Figs. 10 and 11 that at about 10 eV and about 10 keV, η vanishes due to the phase-shift difference going through zero or π. None of the radial dipole matrix elements go through zero at this energy, except for R_5^3 of $n=5$, as we see in Fig. 9.

Deviations from the dipole predictions may be easiest to detect when the dipole correlations vanish. Though this often happens at or around the dipole Cooper minima, the dipole C_{ij} may also vanish away from Cooper minima, being proportional to the dipole parameters in the form $\sum_{i,j} a_{ij}R_iR_j\cos\delta_{ij}/\sum_i b_iR_i^2$, or $\sum_{i,j} a_{ij}R_iR_j\sin\delta_{ij}/\sum_i b_iR_i^2$, as seen in Eqs. (20) and (21). The lowest order corrections to dipole approximation are

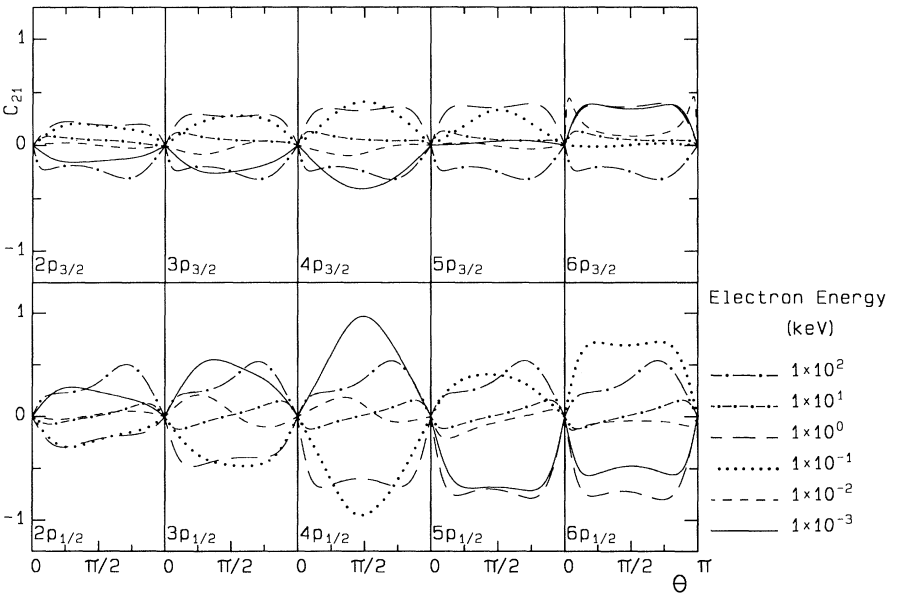

FIG. 5. Full multipole results for C_{21}.

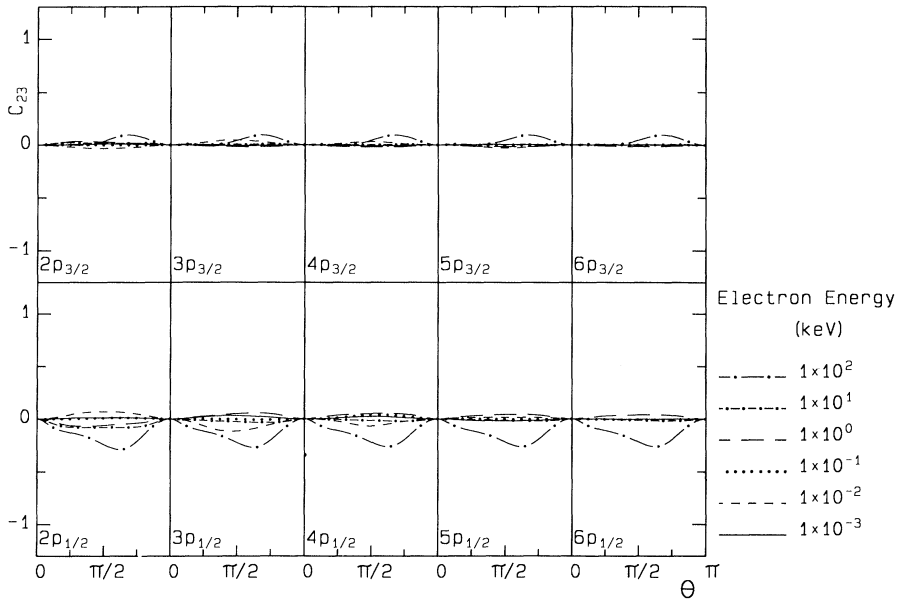

FIG. 6. Full multipole results for C_{23}.

of the form $\sum_{i,j} a_{ij} R_i Q_j \cos\delta_{ij} / \sum_i b_i R_i^2$, where Q_j is a radial quadrupole matrix element (see Refs. 7, 8, 10). For *ns* cases, amplification of the correction terms is observed around the dipole Cooper minima [6], due to a small denominator in the correction term. This is especially true when the separation of the dipole zeros in the two different spin-orbit coupled channels is not too large and no zeros of the quadrupole matrix element or the phase-shift difference term are present near the dipole zeros. For uranium *ns* photoionization, such amplification is suppressed due to the large separation of the dipole zeros [12] and to the presence of nearby quadrupole zeros [5].

For $L>0$, a bigger correction term may be seen when each factor in the numerator of the correction term is large, which usually happens away from the dipole Cooper minima rather than near them. (Although near Cooper minima the denominator as well as the numerator may be small, the denominator for $L>0$ may not be small enough, due to the presence of more dipole channels leading to different partial-wave continuum states.)

We discuss each polarization correlation coefficient separately in the following.

A. C_{02}

C_{02} is the correlation coefficient between unpolarized photons and the spin of the photoelectrons measured in the direction perpendicular to the production plane. It is zero at $\theta=0, \pi/2$, or π for LEOS cases. From Eq. (22) we

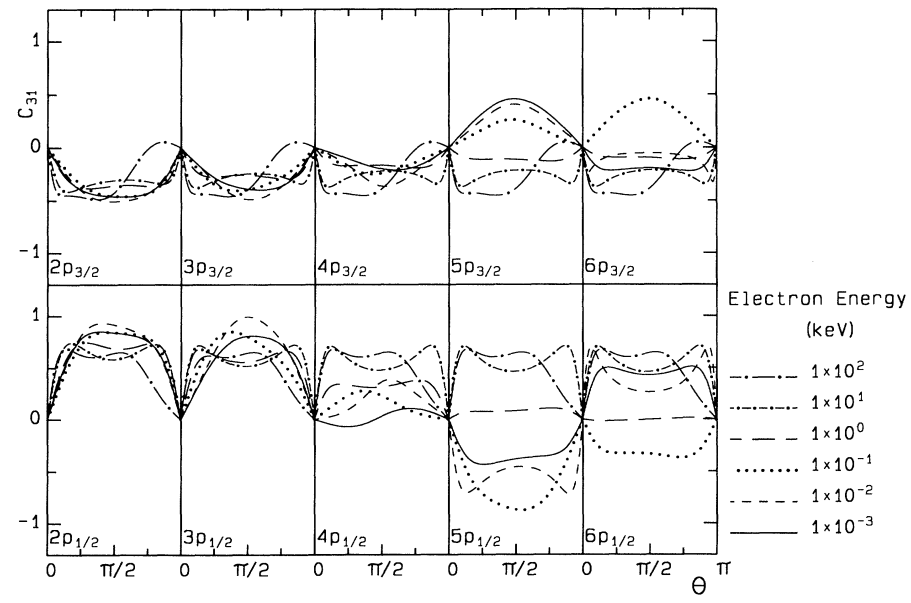

FIG. 7. Full multipole results for C_{31}.

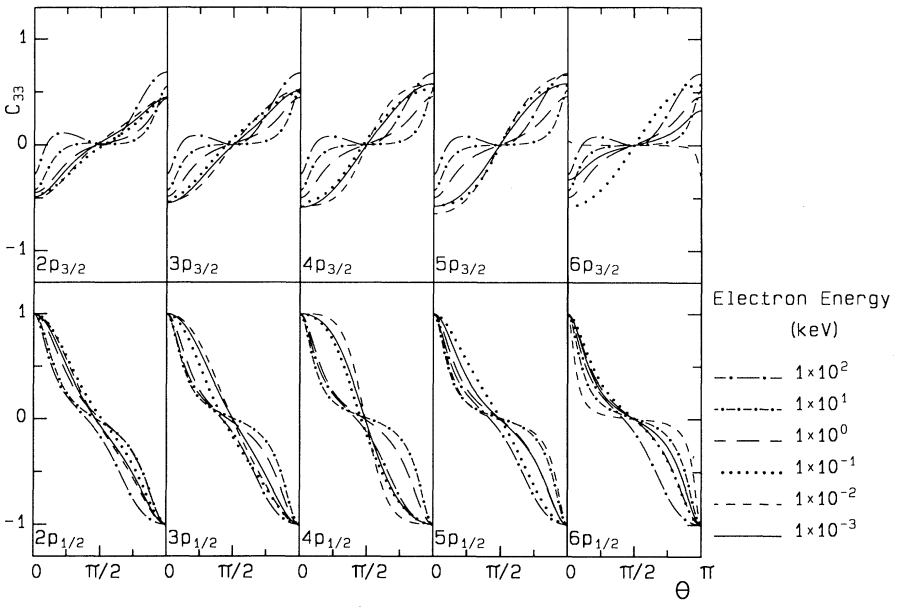

FIG. 8. Full multipole results for C_{33}.

expect, in LEOS cases, that C_{02} for np_J will vanish when η does. We note from Fig. 12 that the deviations from the dipole results are noticeable. As we briefly discussed earlier, $\sin\delta_{13}$ and $\sin\delta_{15}$ go through zero near 10 eV and 10 keV from Fig. 10 and we see that $\sin\delta_{35}\simeq 0$ at all energies studied (note that $\delta_{35}=\delta_{13}-\delta_{15}$ and Fig. 10 shows $\delta_{13}\simeq\delta_{15}$). At $\varepsilon\simeq 10$ eV and 10 keV η goes through zero for all n. Nonzero values of C_{02} at these energies in Figs. 2 and 12 are from the multipole contributions. Above and below these energies the C_{02} curves are completely reversed in sign for all n. For $np_{1/2}$ photoionization, the dipole C_{02} vanishes when R_1^1, R_3^1 (i.e., a dipole Cooper minimum) or $\sin\delta_{13}$ does from Eq. (20). From Fig. 9, we see that $R_3^1=0$ occurs at $\varepsilon\simeq 160$ eV for $n=5$ and at $\varepsilon\simeq 270$ eV for $n=6$. In Fig. 2 C_{02} for $5p_{1/2}$ and $6p_{1/2}$ at 100 eV is reversed in sign compared with C_{02} at 1 keV, confirming the dipole expectations. For $np_{3/2}$, $R_3^3=0$ at $\varepsilon\simeq 60$ eV and $R_5^3=0$ at $\varepsilon\simeq 90$ eV for $n=6$, so that C_{02} for $6p_{3/2}$ at 0.1 keV is close to zero. For $n=5$, there seems to exist a dipole Cooper minimum near threshold both in R_3^3 and R_5^3, leading to vanishingly small η and hence, C_{02} near threshold for $5p_{3/2}$. When $\beta=0$, which can occur at or away from Cooper minima, the denominator of Eqs. (22)–(28) is 1 (isotropic angular distribution) and C_{02} becomes $-\eta\sin\theta\cos\theta$, as seen at 0.1 keV for $6p_{1/2}$ and at 1 eV for $5p_{3/2}$. Note that at Cooper minima η itself may vanish.

At high photon energies, the deviation from the dipole result is large at $\theta=\pi/2$, where the dipole correlation is zero, reflecting the loss of the dipole-type symmetry around $\theta=\pi/2$. At 100 keV a degree of transverse spin polarization of about 30% for $np_{1/2}$ and about 10% along this direction for $np_{3/2}$ is seen in Fig. 12.

B. C_{10}

C_{10} represents the correlation between linear photon polarization in or perpendicular to the production plane and the flux of the photoelectrons detected without measuring their spin. This correlation coefficient for LEOS cases is again zero at $\theta=0$ or π, while it is maximum at $\pi/2$. It is proportional to the asymmetry pa-

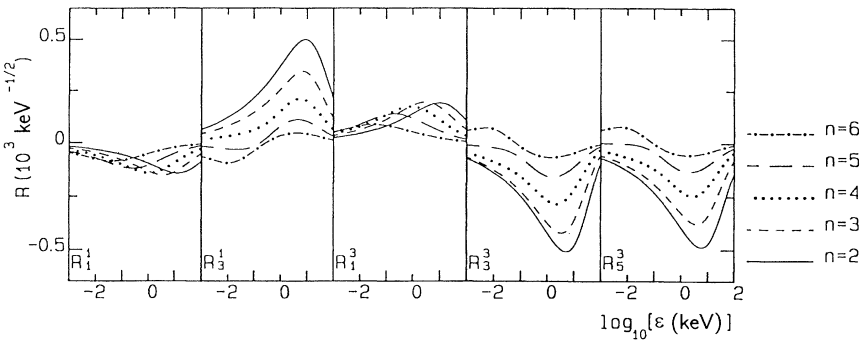

FIG. 9. Radial dipole matrix elements.

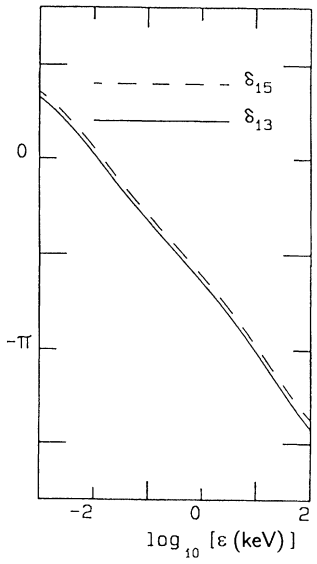

FIG. 10. Phase shift differences.

rameter β of the usual angular distribution for photoelectrons without a spin measurement. Therefore it will vanish when the angular distribution is isotropic. Smallness of C_{02} for $4p_{3/2}$ and $5p_{3/2}$ near threshold and for $6p_{3/2}$ at around 100 eV, as well as the sign reversal for $4p_{1/2}$, $4p_{3/2}$, and $5p_{3/2}$ between 100 eV and 1 keV, and the absence of the sign reversal for other cases from Fig. 3 are all related to the sign changes of β in Fig. 11. At 1 keV, we see a merging of β for all np_J cases and the C_{10} curves are almost identical at this energy.

C. C_{12}

C_{12} is the correlation between the linear photon polarization in or perpendicular to the production plane and the spin polarization of the photoelectrons measured perpendicular to the production plane. As for *ns* photoionization, we see almost the same features for C_{12} as for C_{02}, except at the highest energy studied for $np_{1/2}$ at backward angles, which can be barely seen in comparing Figs. 2 and 4 (and also Figs. 12 and 14, since C_{12} and C_{02} are identical in dipole approximation).

D. C_{21}

This correlation is for transversely polarized photoelectron spin in the production plane produced by photons linearly polarized at $\pm\pi/4$ from the production plane. From Eqs. (22), (24), and (25), we see that for LEOS cases C_{21} differs from C_{12} or C_{02} by a factor of $\cos\theta$, and the variation in energy can be understood similarly.

E. C_{23}

In the dipole approximation, this correlation coefficient, which is for longitudinal spin polarization with photons linearly polarized at $\pm\pi/4$ from the production plane, is identically zero. We see deviations com-

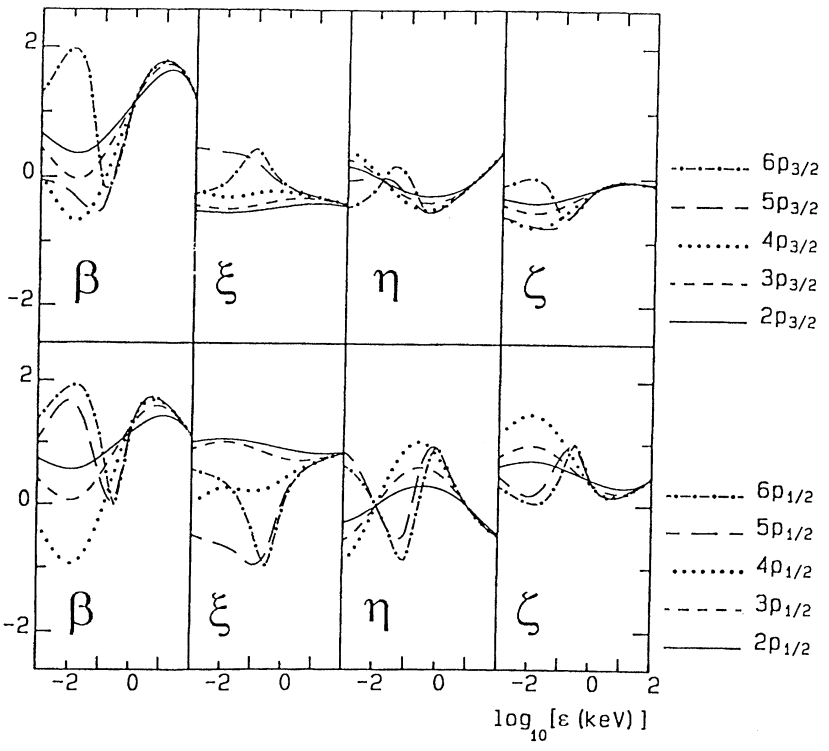

FIG. 11. Dipole parameters.

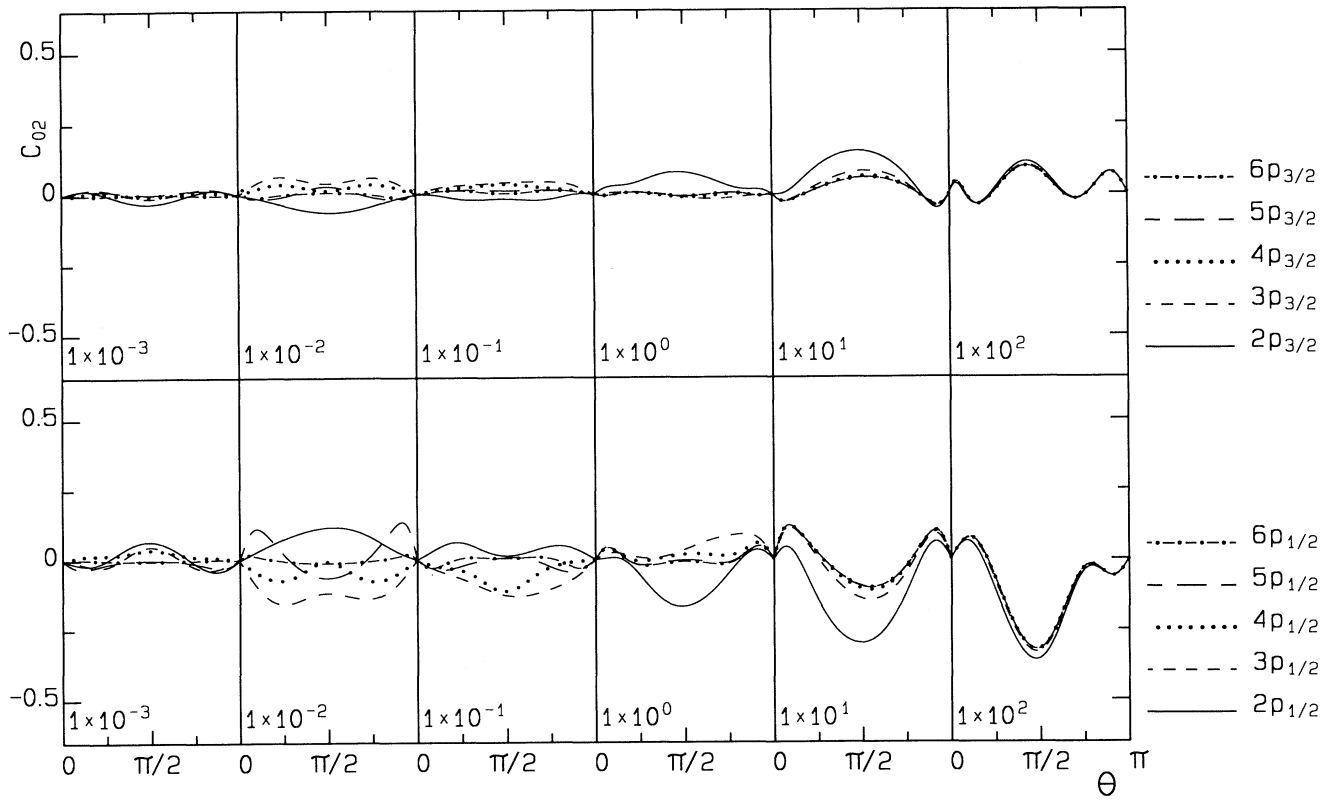

FIG. 12. Differences of full multipole results from the dipole case for C_{02}.

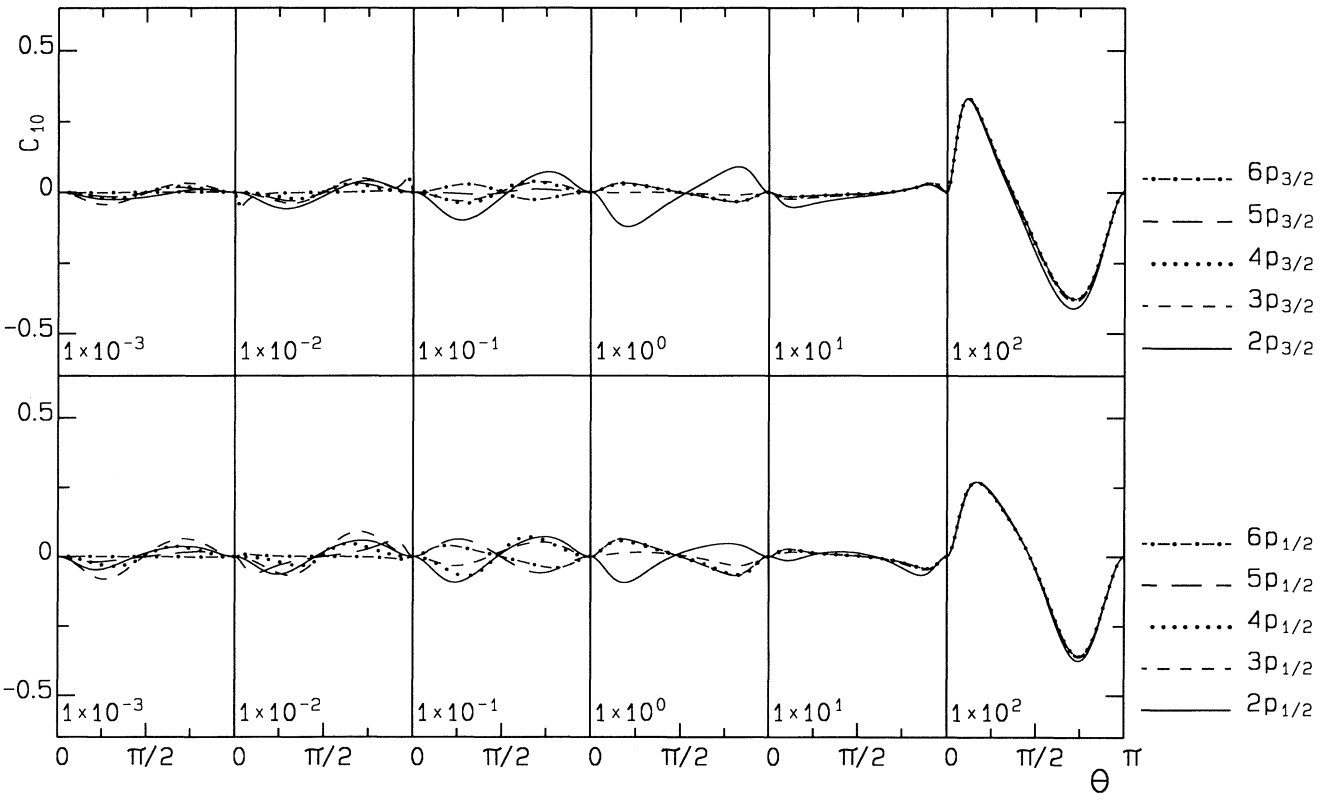

FIG. 13. Differences of full multipole results from the dipole case for C_{10}.

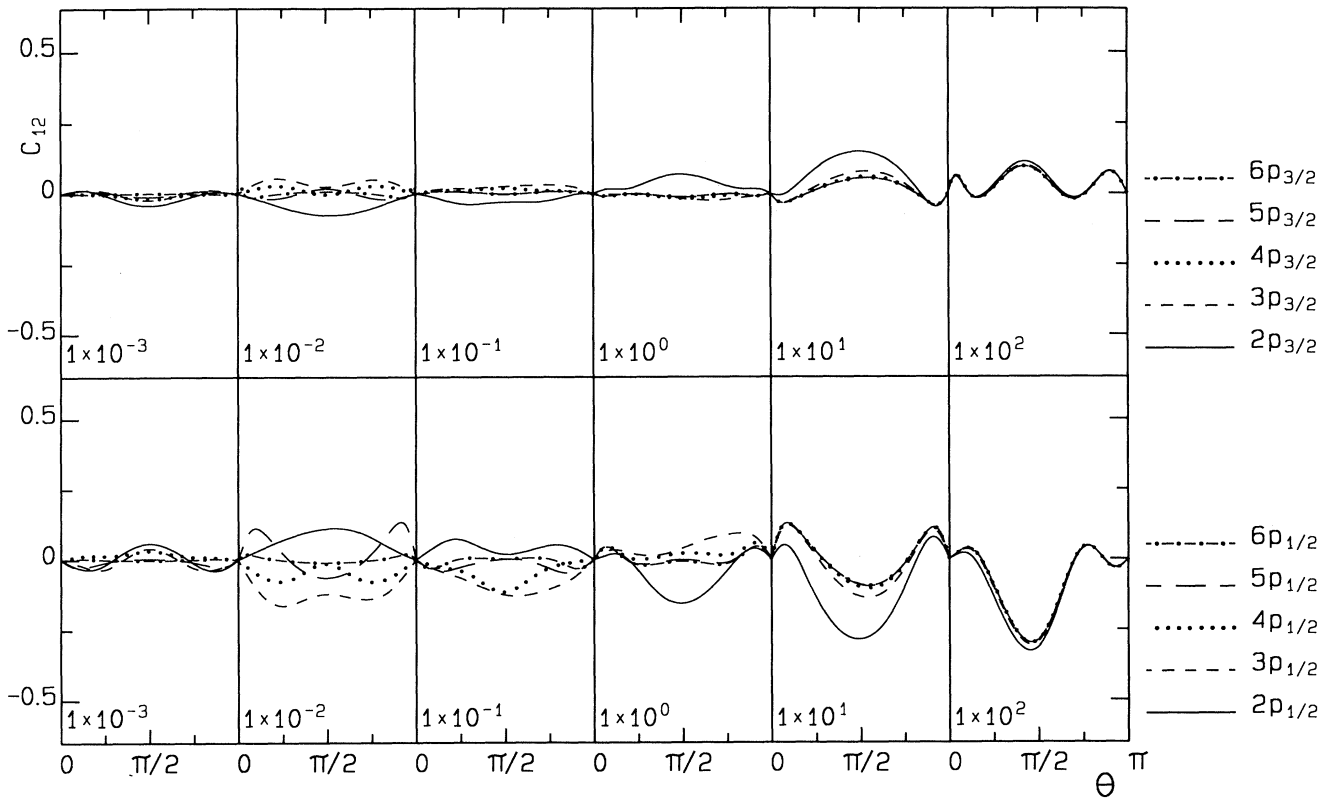

FIG. 14. Differences of full multipole results from the dipole case for C_{12}.

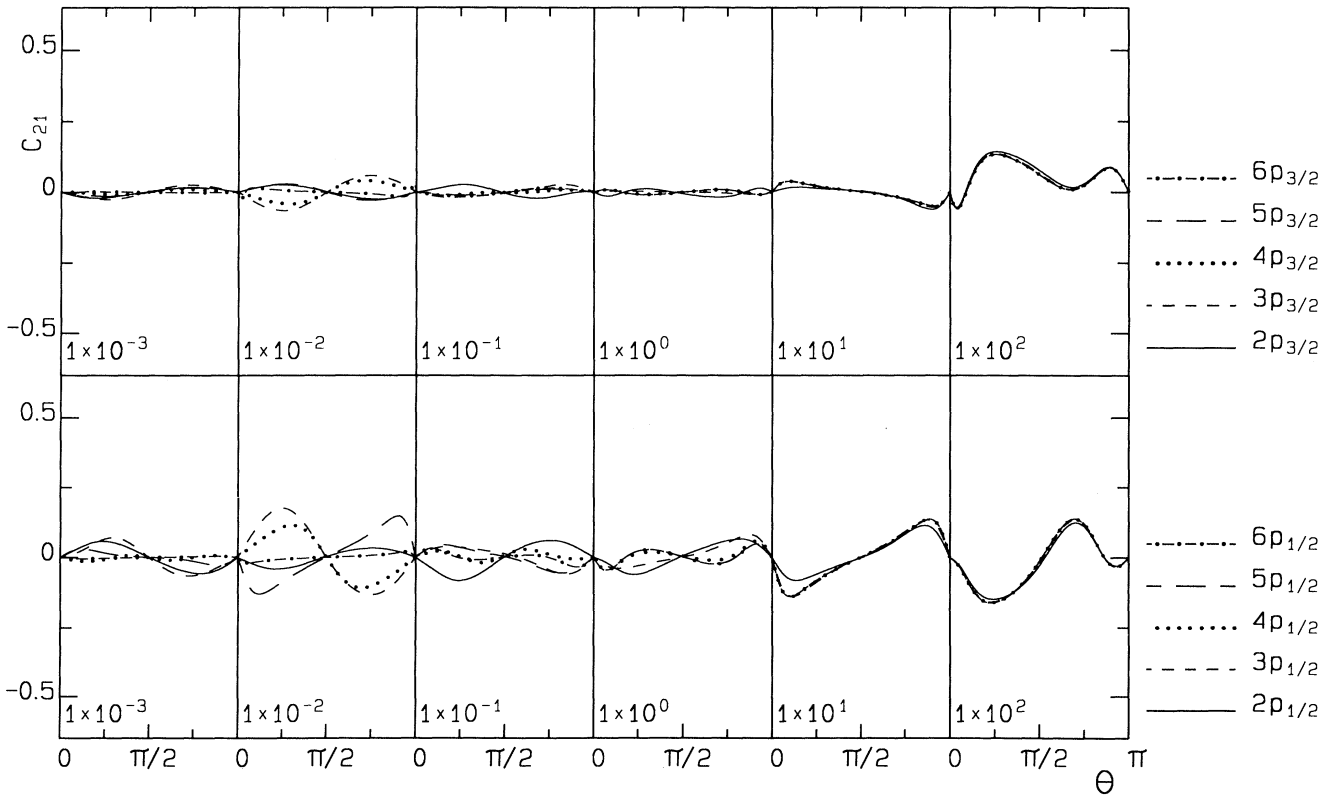

FIG. 15. Differences of full multipole results from the dipole case for C_{21}.

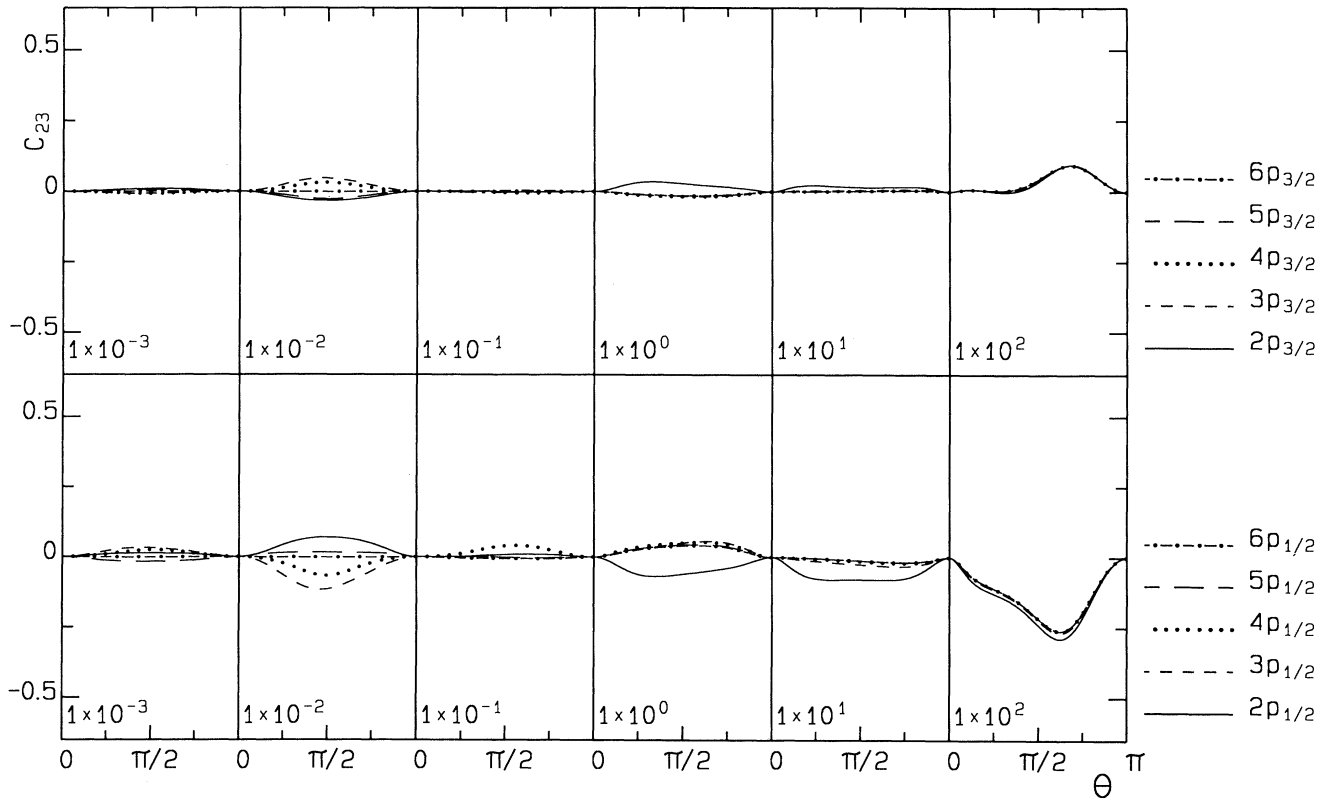

FIG. 16. Differences of full multipole results from the dipole case for C_{23}.

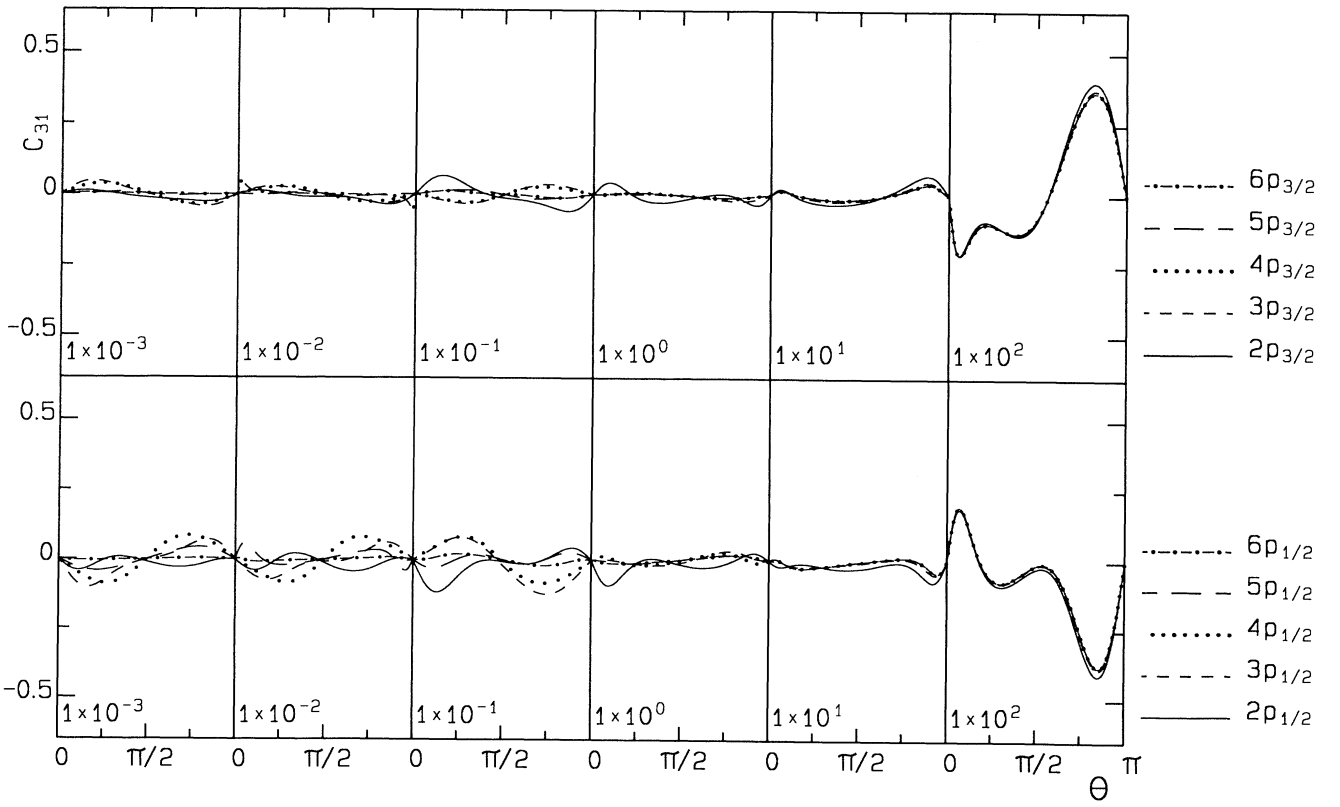

FIG. 17. Differences of full multipole results from the dipole case for C_{31}.

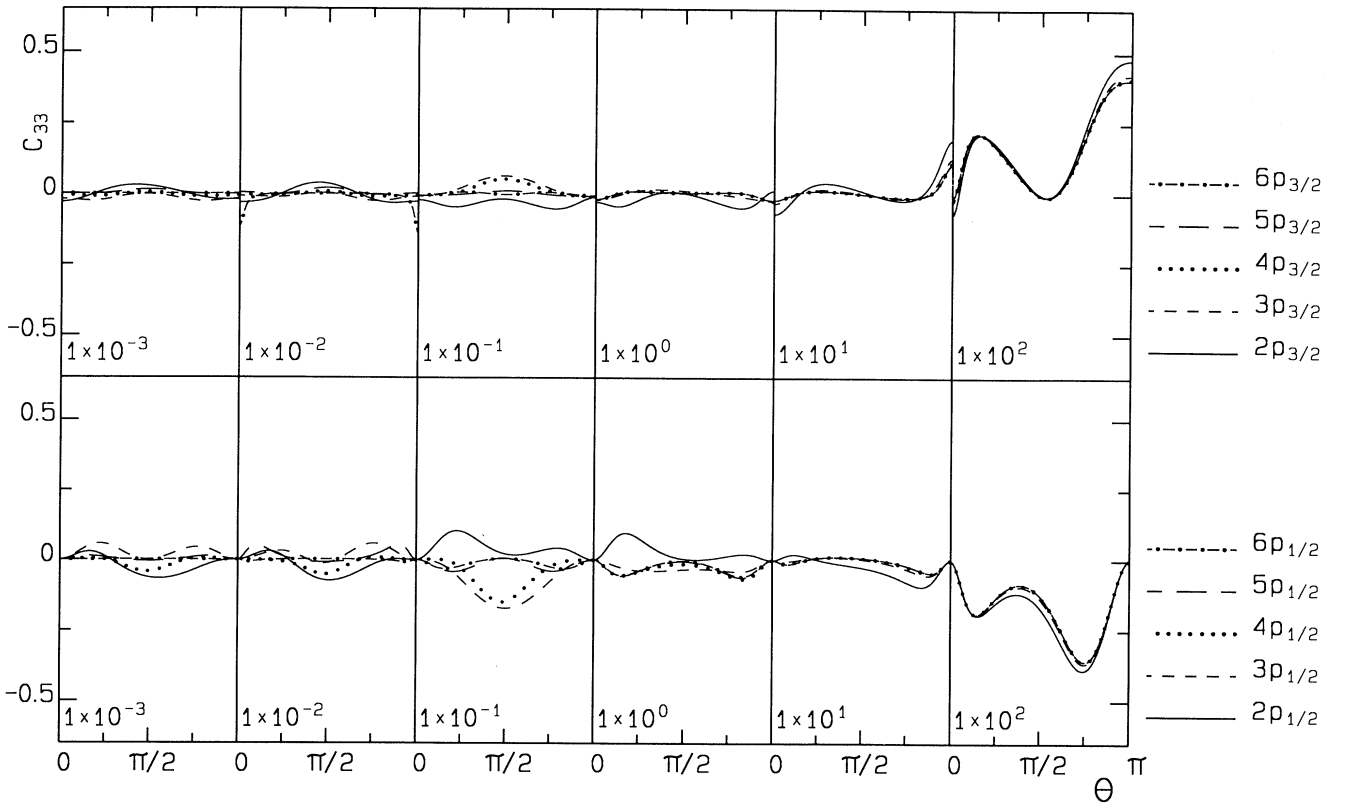

FIG. 18. Differences of full multipole results from the dipole case for C_{33}.

ing from multipole contributions, which are small in LEOS cases, except at 10 eV. At 100 keV our multipole results indicate more than 25% spin polarization at a slightly backward angle.

F. C_{31}

With circularly polarized photons, photoelectron spin polarization can be either longitudinal or transverse in the production plane (helicity transfer). This correlation coefficient is for transverse spin polarization. For LEOS cases $C_{31}=0$ when $\xi=0$, which is the case with $\varepsilon\simeq1$ keV for $6p_{3/2}$ in Fig. 7 (and for $\varepsilon\simeq0.3$ keV for $5p_{3/2}$).

Note again that for $np_{1/2}$ cases, when $\beta=0$ and $C_{31}=-\sin\theta$ and the initial photons are circularly polarized, a degree of photoelectron spin polarization approaching unity may be observed for a spin direction making an angle θ with the $\hat{3}$ axis (2θ with the $\hat{z}$ axis) in the production plane which, as we have previously discussed, occurs for $n=5$ and 6.

G. C_{33}

The correlation coefficient C_{33} for longitudinal spin polarization and circularly polarized photons is the only nontrivially nonzero correlation at $\theta=0$ or π, though it vanishes at all angles when $\xi=0$ for LEOS cases, as occurs at 10 keV for $6p_{3/2}$. As discussed in the previous subsection, at energies where $\beta=0$ and $C_{33}=\cos\theta$, the photoelectrons from $np_{1/2}$ with circularly polarized photons are expected to be fully polarized along the spin direction making an angle θ with the $\hat{3}$ axis.

ACKNOWLEDGMENTS

This research was supported in part by the U.S. National Science Foundation under Grant No. PHY 90 05763. Y. S. Kim gratefully acknowledges the support of Center for Molecular Science at KAIST, KOSEF Grant No. 911-0204-031-2 and the U.S. National Science Foundation through a grant for Theoretical Atomic and Molecular Physics at Harvard University and the Smithsonian Astrophysical Observatory.

[1] Young Soon Kim, I. B. Goldberg, and R. H. Pratt, Phys. Rev. A **45**, 4542 (1992).

[2] R. H. Pratt, Akiva Ron, and H. K. Tseng, Rev. Mod. Phys. **45**, 273 (1973).

[3] R. H. Pratt, R. D. Levee, R. L. Pexton, and W. Aron, Phys. Rev. **134**, A916 (1964).

[4] Akiva Ron, R. H. Pratt, and H. K. Tseng, Chem. Phys. Lett. **47**, 377 (1977); H. K. Tseng, R. H. Pratt, Simon Yu,

and Akiva Ron, Phys. Rev. A **17**, 1061 (1978).
[5] Young Soon Kim, R. H. Pratt, Akiva Ron, and H. K. Tseng, Phys. Rev. A **22**, 567 (1980).
[6] M. S. Wang, Y. S. Kim, R. H. Pratt, and A. Ron, Phys. Rev. A **25**, 857 (1982).
[7] A. Bechler and R. H. Pratt, Phys. Rev. A **39**, 1774 (1989); **42**, 6400 (1990).
[8] R. H. Pratt and Young Soon Kim, Romanian, J. Phys. **38**, 353 (1993).
[9] K. N. Huang, Phys. Rev. A **22**, 223 (1980).
[10] J. W. Cooper, Phys. Rev. A **47**, 1841 (1993); see also Phys. Rev. A **42**, 6942 (1990), but note erratum **45**, 3362(E) (1992).
[11] N. Böwering, M. Salzmann, M. Müller, H.-W. Klausing, and U. Heinzmann, Phys. Scr. **41**, 429 (1981).
[12] Young Soon Kim, Akiva Ron, R. H. Pratt, B. R. Tambe, and S. T. Manson, Phys. Rev. Lett. **46**, 1326 (1981).